Sensing and Bio-Sensing Research 13 (2017) 49–54

Contents lists available at ScienceDirect

Sensing and Bio-Sensing Research

journal homepage: www.elsevier.com/locate/sbsr

Effect of biomolecule position and fill in factor on sensitivity of a Dielectric Modulated Double Gate Junctionless MOSFET biosensor

Ehsanur Rahman *, Abir Shadman, Quazi D.M. Khosru

Department of Electrical and Electronic Engineering, Bangladesh University of Engineering and Technology, Dhaka-1000, Bangladesh

ARTICLE INFO

Article history:
Received 11 November 2016
Received in revised form 7 February 2017
Accepted 10 February 2017
Available online xxxx

Keywords:
Junctionless FET
Nanobiosensor
Biomolecule
Double Gate
Sensitivity

ABSTRACT

In this work, the performance of Junctionless Double Gate MOSFET for the label-free electrical detection of biomolecules like enzyme, cell, DNA, etc. has been investigated with the help of an analytical model. The impact of neutral biomolecules on the electrical characteristics of n-type Si Junctionless Double Gate MOSFET has been analyzed under dry environment situation. The change in the threshold voltage has been used as the sensing metric to detect the sensitivity of the mentioned device architecture for biomolecule detection. Biomolecule position and their fill in factor of the sensing site have been investigated to find out their effect on sensitivity. Moreover, the effect of drain bias on sensitivity has been found to be a crucial factor for the optimization of biosensor's detection capability.

1. Introduction

Currently available technology for detecting tumor markers, antigen-antibody complexes, and pathogens is complex, time-consuming and expensive [1,2]. FET-based biosensors have emerged as a potential candidate in the label-free detection of biomolecules like cancer biomarkers, Protein, DNA and other pathogens in a cost efficient and reliable way, an alternative to optical detection technique. The first concept of electronic pH sensing with ion-sensitive field effect transistors (ISFETs) was suggested by Bergveld [3]. The pH sensitivity (mV/pH) of a conventional single-gated ISFET is defined by the changes of threshold voltage (V_T) at a given amount of pH changes. However, such sensitivity is limited to Nernst limit of 59 mV/pH. To overcome the Nernst limit of sensitivity in single-gated ISFET, recent literature [4–7] has suggested double-gated field effect transistors. A modified version of ISFETs has also been used to detect biomolecules like DNA, Protein, and biomarkers indicative of various diseases. However, there are several problems in detecting biomolecule reliably using ISFET. First of all, the electrical signals from the ISFET biosensor depend on the ionic concentration of the sample solution [8] which is characterized by Debye length. Second, various ionic levels of the sample can significantly change the electrical signal of ISFET biosensors [9]. Third, controlling the ionic concentration accurately of any real human sample, such as blood serum, urine or saliva is difficult [10]. Moreover, the conductance modulation in the FET sensor is caused by the interaction potential and this potential might get partially screened by the high ionic strength of the buffer solution. This screening directly depends on the Debye–Hückel length [10]. Therefore, Debye-screening-free sensors working under the dry environment can provide several advantages over electrolyte-based biosensors. In the present work, Junctionless Double Gate (JL-DG) MOSFET under dry environment condition [11] has been investigated for its application as a biosensor for the label-free electrical detection of the biomolecules. Fabrication feasibility of Nanowire Junctionless MOSFET (JL-MOSFETs) has been already demonstrated by Colinge et al. [12,13]. Immunity to many Short Channel Effects (SCEs) like DIBL, improved on state and transfer characteristics have made JL-MOSFETS more advantageous over their conventional counterparts like junction based FETs [14,15]. Therefore, JL-DG MOSFET with cavity regions functionalized for detecting biomolecule in a dry environment can be a viable solution to the problems associated with biomolecule sensing under aqueous electrolyte condition. In dielectric modulated field-effect transistor (DM-FET), the insulator layer is etched to create a nanogap region underneath the gate material. DM-FET is capable of detecting even neutral biomolecules, which is not possible with conventional ISFET based biosensor. DM-FET based sensor also shows excellent compatibility with standard CMOS process [16–18]. In our work, we have extended the model widely used in the literature [11, 19–23] to incorporate the effect of the position of the biomolecule and their percentage coverage in the sensing site on sensor's performance. The analytical equations governing the electrostatic potential and current in different regions of the biosensor used in this work are briefly described in the following section. Despite the analytical model available in the recent literature, this work is unique in a sense that there has been no report regarding the effect of biomolecules position and percentage coverage of the cavity on the performance of such biosensor

* Corresponding author.
E-mail address: Ehsaneee@eee.buet.ac.bd (E. Rahman).

http://dx.doi.org/10.1016/j.sbsr.2017.02.002

in a dry environment according to the authors' best knowledge. Moreover, the findings of this work have an immediate practical impact due to two reasons. First of all, it has been demonstrated experimentally that even under the precisely controlled experiments, the complete fill-in is hard to achieve [24]. Secondly, in a practical situation, the capture of biomolecules can be asymmetric, random and quite complex due to low binding probability in a carved nanogap [25]. Hence, along with the fill-in factor, the possible location of biomolecule binding site within the nanogap (cavity) can differ, therefore, should be analyzed. Therefore, the study of the biosensor with partially filled and randomly distributed biomolecule can provide valuable insight to the dependence of sensitivity on biomolecule's position and percentage fill in of nanogap cavity region. Though modeling schemes focused on biosensing using DM-FET are available in the literature, such modeling does not incorporate the practical consideration of randomly distributed biomolecule in sensing sites. In real life application, bio-molecules can be located at any position in the cavity. In this work, we investigate this unexplored field of potentiometric biosensing in a dry environment with a view to understand and explain the effect of the partially filled cavity on biosensor's performance and their implication in practical application. To model the real life situation, we have created three different cavities in gate oxide region as shown in Fig. 1(a). We have considered different cases like-

i). Cavity regions on both sides of the gate oxide are filled with bio-molecule.
ii). Any two of the cavities are filled with bio-molecule, the other one is empty (filled with air)
iii). Any one of the cavities is filled, other two are empty.

Though the results presented in this study is a small subset of the real life situation, our extended analytical model developed in this work can take into account of any distribution profile of the biomolecules simply by changing the length and dielectric permittivity of different cavity regions.

2. Device structure

The device architecture for n-type Si Junctionless Dielectric Modulated Double Gate MOSFET (JL-DM-DG-MOSFET) based biosensors used in this work is depicted in Fig. 1(a). Here, L_1, L_3, and L_4 are the lengths of the nanogap cavity; L_2 is the length of the gate oxide SiO_2. T_{bio}, T_{ch}, T_{ox} are the thickness of the nanogap cavity, channel and gate oxide respectively. For first structure, the typical values of different parameters used here are T_{bio}/T_{ox} = 9 nm (plus 1 nm Native SiO_2), T_{ch} = 10 nm, L_1 = 10 nm, L_2 = 30 nm, $L_3 = L_4$ = 5 nm. Nanogap surfaces are properly functionalized for the immobilization of biomolecules. As a result, sensing sites are formed in nanogap cavity regions that can detect the target biomolecules. The surface potential from extended analytical modeling of this study was verified with reasonable accuracy as shown in Fig. 1(b) by comparing it with simulation results from 'Silvaco Atlas', which is commonly used to characterize the electrical properties of the semiconductor devices [26]. Various biomolecules have different dielectric constant (for e.g. streptavidin = 2.1 [27], protein = 2.50, biotin = 2.63 [28], and APTES = 3.57 [29]) [30]. So, the presence of the neutral biomolecules in the nanogap cavity can be simulated by introducing material having dielectric constant ($\epsilon_{bio} > 1$) corresponding to biomolecules in the nanogap cavities (assuming that the cavities are completely or partially filled with biomolecules). Before biomolecule immobilization, the nanogap cavity is filled with surrounding air (dielectric constant, $\epsilon_{air} = 1$). The presence of biomolecules in the nanogap cavity region can be simulated by defining an oxide layer with height of T_{bio} = 9 nm and varying its dielectric constant ϵ_{bio} = 2, 3, 4, 5, 7. The height/thickness of the layer is chosen to resemble the practical height of the biomolecules [27,29].

3. Analytical model development

To obtain an analytical expression for potential distribution and drain current, the channel is divided into four regions as follows:

$$\text{Region I}: 0 \le x \le t_{si}, 0 \le y \le L_1 \tag{1}$$

$$\text{Region II}: 0 \le x \le t_{si}, L_1 \le y \le L_1 + L_2 \tag{2}$$

$$\text{Region III}: 0 \le x \le t_{si}, L_1 + L_2 \le y \le L_1 + L_2 + L_3 \tag{3}$$

$$\text{Region IV}: 0 \le x \le t_{si}, L_1 + L_2 + L_3 \le y \le L_1 + L_2 + L_3 + L_4 \tag{4}$$

Potential distribution is obtained by solving the Poisson's equation separately in each region as follows:

$$\frac{\partial^2 \phi_i(x,y)}{\partial x^2} + \frac{\partial^2 \phi_i(x,y)}{\partial y^2} = -\frac{qN_d}{\varepsilon_{si}} \tag{5}$$

where i = 1, 2, 3, 4 for region 1, 2, 3 and 4, respectively. $\phi_i(x,y)$ is the *2-D* potential distribution in the silicon channel, N_d is the doping in the silicon channel, q is the electron charge, t_{si} is the channel thickness and ε_{si} is the dielectric permittivity of silicon. Using parabolic approximation and relevant boundary conditions, we can convert the differential Eq. (5) to the form

$$\frac{\delta \phi_{mi}(y)}{\delta y^2} - \frac{\varphi_{mi}(y) - V_{gs} + V_{fbi}}{\eta_i^2} = -\frac{qN_d}{\varepsilon_{si}} \tag{6}$$

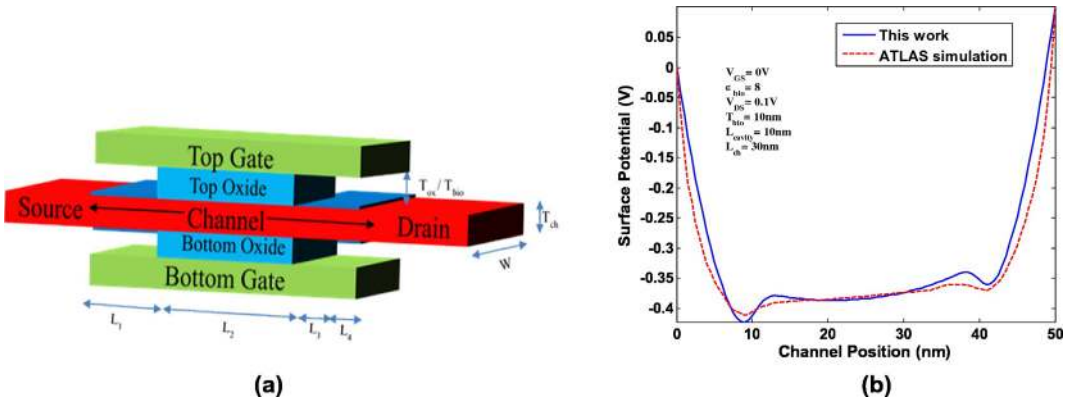

Fig. 1. (a) Schematic initial structure of Junctionless DM-DG-MOSFET biosensor. Different parameters considered here are as follows, T_{bio}/T_{ox} = 9 nm, with 1 nm SiO_2 considered on both side of the channel in the cavity regions. T_{ch} = 10 nm, L_1 = 10 nm, L_2 = 30 nm, $L_3 = L_4$ = 5 nm. Doping in the source, drain, and the channel is 1×10^{25} m^{-3}. (b) Comparison of surface potential obtained from analytical model and ATLAS simulation for the device in (a).

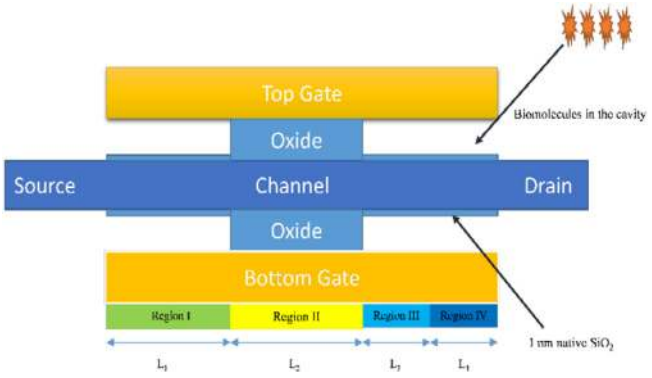

Fig. 2. 2D view (side) of Fig. 1(a). Here Region IV is connected to drain.

where

$$\eta_i = \sqrt{\frac{4\varepsilon_{si}t_{si} + C_i{t_{si}}^2}{8C_i}}$$

where C_i is the gate capacitance per unit area of the gate dielectric of JL-DM-DG-MOSFET in different region of the channel. V_{gs} and V_{fbi} are gate to source voltage and flat band potential respectively. The solution of the differential Eq. (6) can be written in the form

$$\varphi_{mi}(y) = A_i e^{\frac{y}{\eta_i}} + B_i e^{-\frac{y}{\eta_i}} + \sigma_i \tag{7}$$

where

$$\sigma_i = -{\eta_i}^2 \frac{qN_d}{\varepsilon_{si}} - (V_{gs} - V_{fbi})$$

In Eqs. (6) and (7), $\varphi_{mi}(y)$ is the mid-channel potential in different regions and it is related to surface potential $\varphi_{fsi}(y)$ in the channel through the following equation.

$$\varphi_{mi}(y) = \varphi_{fsi}(y) + \frac{C_i t_{si}}{4\varepsilon_{si}}\left(\varphi_{fsi}(y) + V_{gs} - V_{fbi}\right) \tag{8}$$

Constant A_i and B_i are obtained by solving the boundary conditions at the source and drain junctions.

Solving boundary conditions, we get

$$B_1 = \frac{(V_{bi} - \sigma_1)e^{\frac{L_1}{\eta_1}} - (\psi_1 - \sigma_1)}{2\sinh\left(\frac{L_1}{\eta_1}\right)} \tag{9}$$

$$A_1 = V_{bi} - \sigma_1 - B_1 \tag{10}$$

$$B_2 = \frac{(\psi_1 - \sigma_2)e^{\frac{L_2}{\eta_2}} - (\psi_2 - \sigma_2)}{2\sinh\left(\frac{L_2}{\eta_2}\right)e^{-\frac{L_1}{\eta_2}}} \tag{11}$$

$$A_2 = \frac{\psi_1 - \sigma_2 - B_2 e^{-\frac{L_1}{\eta_2}}}{e^{\frac{L_1}{\eta_2}}} \tag{12}$$

$$B_3 = \frac{(\psi_2 - \sigma_3)e^{\frac{L_3}{\eta_3}} - (\psi_3 - \sigma_3)}{2\sinh\left(\frac{L_3}{\eta_3}\right)e^{-\frac{(L_1+L_2)}{\eta_3}}} \tag{13}$$

$$A_3 = \frac{\psi_2 - \sigma_3 - B_3 e^{-\frac{(L_1+L_2)}{\eta_3}}}{e^{\frac{(L_1+L_2)}{\eta_3}}} \tag{14}$$

$$B_4 = \frac{(\psi_3 - \sigma_4)e^{\frac{L_4}{\eta_4}} - (V_{bi} + V_{ds} - \sigma_4)}{2\sinh\left(\frac{L_4}{\eta_4}\right)e^{-\frac{(L_1+L_2+L_3)}{\eta_4}}} \tag{15}$$

$$A_4 = \frac{\psi_3 - \sigma_4 - B_4 e^{-\frac{(L_1+L_2+L_3)}{\eta_4}}}{e^{\frac{(L_1+L_2+L_3)}{\eta_4}}} \tag{16}$$

Here V_{bi} is the built-in potential. ψ_1, ψ_2 and ψ_3 are the intermediate potentials, obtained by maintaining continuity of the potential and lateral electric field at the interface of each region.

After solving $\varphi_{mi}(y)$, we can obtain the 2D potential anywhere in the channel using the equation

$$\varphi_i(x,y) = \varphi_{fsi}(y) + \frac{C_i}{\varepsilon_{si}}\left(\varphi_{fsi}(y) - V_{gs} + V_{fbi}\right)x - \frac{C_i}{\varepsilon_{si}t_{si}}\left(\varphi_{fsi}(y) - V_{gs} + V_{fbi}\right)x^2 \tag{17}$$

Drain current in the subthreshold region is achieved by using the expression of potential from Eq. (17), and is given by

$$I_D = \frac{W\mu kT\left(1 - \exp\left(-\frac{V_{ds}q}{kT}\right)\right)}{\sum_{i=1}^{4}\int_0^{L_i}\frac{1}{\int_0^{t_{si}} n_i \exp\left(\frac{\phi_i(x,y)q}{kT}\right)dx}dy} \tag{18}$$

Here V_{ds} is the drain to source voltage, μ is the channel mobility, n_i is the intrinsic carrier density in the channel, T is the temperature in kelvin, k is Boltzmann constant and q is the charge of an electron.

4. Working principle of the device

For sensing biomolecules, nanogap cavity regions are formed in the gate oxide of the device which can immobilize the target biomolecules with proper surface functionalization. In the absence of target biomolecules, nanogap cavity regions are filled with air. So dielectric constant of the cavity region is different from that of the gate oxide in Region II ($L_2 = 30$ nm). When target biomolecules (like Streptavidin, Biotin,

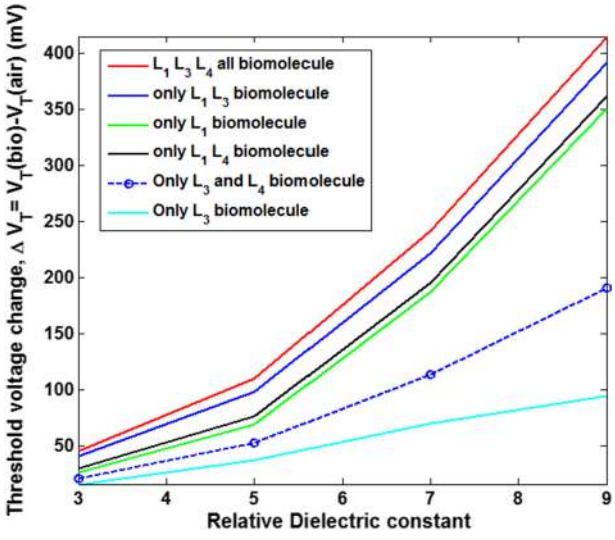

Fig. 3. Variation of sensitivity factor ΔV_{th} for n-type DM-DG-MOSFETs for different positions of biomolecule in the cavity region when Region IV is connected to drain.

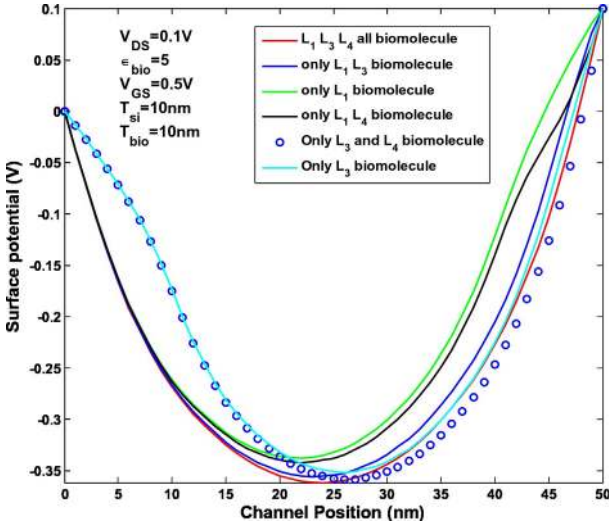

Fig. 4. Effect of biomolecule position and fill in factor in the cavity region on surface potential when Region IV is connected to drain.

Avidin, enzyme, cell, DNA, APTES) are immobilized in the nanogap of the cavity region, the dielectric constant changes and the gate capacitance of the device changes. Consequently, electrical characteristics of the device, such as drain current and threshold voltage will vary according to the dielectric constant of the target biomolecules [22].

5. Results and discussions

5.1. Variation of sensitivity with position of biomolecule

In this work, we have investigated the effect of biomolecule's position on the threshold voltage of the device, therefore, sensitivity to detect biomolecule. We have used the device shown in Fig. 1(a) where it is possible to fill the cavity region partially with biomolecule and the region left is to be occupied by air. Such an arrangement of biomolecules can offer a real insight to effect of fill in factor on device's sensitivity. We also study the spatial variation of partially filled biomolecule to determine whether such variations yield a better sensitivity or not. To investigate those critical effects of biomolecule position and fill in factor in cavity region on sensitivity, the entire oxide layer is divided into four separate regions as shown in Fig. 1(a). In this study, we have set the dimensions of those four regions as $L_1 = 10$ nm, $L_2 = 30$ nm, $L_3 = 5$ nm and $L_4 = 5$ nm. Region II ($L_2 = 30$ nm) is kept as a fixed oxide layer whereas Region I, III and IV work as a cavity for biomolecule's

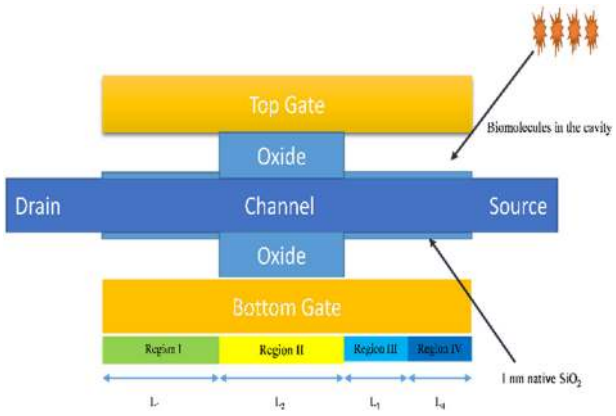

Fig. 6. 2D view (side) of Fig. 1. Here Region I is connected to drain.

placement. These three regions can be either filled with biomolecules or kept empty. It will result in different possible cases based on the presence or absence of biomolecule. Moreover, depending on whether Region I or Region IV is connected to the drain, each variation of the position of biomolecule will result in two different configurations of biomolecule's distribution in the cavity sites. Here we define sensitivity as

$$\Delta V_{th} = V_{th}(\epsilon_{bio}) - V_{th}(\epsilon_{air})$$

5.2. Dependence of sensitivity on Biomolecule's position when Region IV is connected to drain

In this particular configuration, a drain voltage is applied to Region IV (as shown in Fig. 2) with respect to the source. Here source is connected to Region I. Any one of the regions I, III and IV can be filled with biomolecules of different dielectric constants. The sensitivity (change in threshold voltage after the insertion of biomolecules with different dielectric constants) of the various possible placements of the biomolecule is shown in Fig. 3. As shown in Fig. 3, the best sensitivity is obtained when the entire cavity regions (region I, III and IV) are filled with biomolecules. This is logical since higher the fill in factor of a biomolecule in the cavity region, better its influence is on device current. Hence, it will result in a greater change in threshold voltage of the device compared to the 'no biomolecule' case. Using similar reasoning it can be predicted that the next highest sensitivity can be obtained when only Region III or Region IV is empty and all other cavity regions

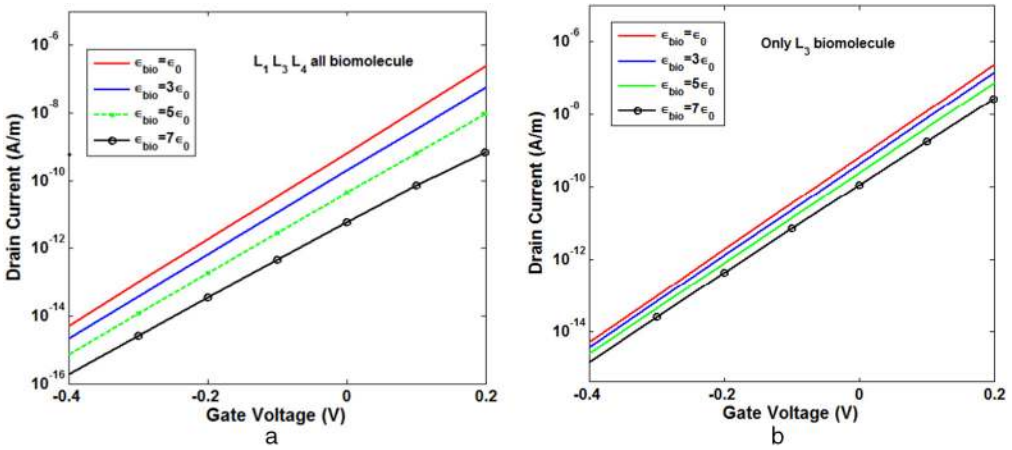

Fig. 5. Effect of biomolecule position and fill-in factor in the cavity region on drain current in the sub-threshold region. Here region IV is connected to drain. The spread of the drain current in the sub-threshold region increases with fill in factor, which results in a higher change in threshold voltage. (a) is for 100% fill-in factor (b) is for 25% fill-in factor.

are filled with biomolecules. Results shown in Fig. 3 actually support this prediction. However, an interesting observation from Fig. 3 is that for a similar percentage of biomolecule coverage, the case in which biomolecules are more closely distributed to the center of the channel will yield better sensitivity. So, the case in which only L_4 (Region IV) is empty (of biomolecule) will result in a higher sensitivity than the case in which only L_3 (Region III) is empty.

A reasonable explanation of such finding is, as the biomolecules get closer to the center of the channel, the gate voltage exerts a higher influence on channel potential barrier through capacitive coupling effect of the biomolecule. Hence, such distribution of biomolecule will result in a higher change in drain current with a variation of biomolecule's dielectric constant. All other phenomena observed in Fig. 3 can be explained by the similar reasoning described above. Fig. 4 shows the surface potential along the channel direction for a different combination of biomolecule's position and their percentage of fill in factor of the cavity region. From Fig. 4 it is evident that changing the biomolecule position considerably skews the potential profile along the channel direction. It can also be observed from Fig. 4 that the portion of the channel over which biomolecule is present in the cavity region has a lower surface potential compared to the part free from biomolecule. Fig. 5 shows the sub-threshold current for two different cases of biomolecule occupancy in the cavity for various dielectric constants of the biomolecule. As can be seen from Fig. 5, with a fill in factor of 100%, current in sub-threshold region is more widely spread compared to a fill in factor of 25%. A higher spread in drain current implies a higher change in threshold voltage hence greater sensitivity to the change in dielectric constant. Therefore, in summary, we can draw the following conclusions from the variation of biomolecule fill in factor and position in the cavity region-

- The greater the fill in factor of a biomolecule, higher the sensitivity of the DG-FET in detecting biomolecule.
- The more closely located the biomolecules to the center of the channel; better the sensitivity of the biosensor.
- The higher the dielectric constant of the biomolecule, greater its effect on sensitivity.

5.3. Dependence of sensitivity on position of biomolecule when Region I is connected to drain

In a slightly different configuration, we can connect Region I (as shown in Fig. 6) to the drain side and Region IV (as shown in Fig. 6) can be attached to the source side. The dimensions of various regions are similar to that of the previous configuration. Our main purpose in this part is to investigate the effect of Drain to Source voltage on the sensitivity of the device along with the variation of biomolecule's position and percentage of area coverage.

From Fig. 7, it can be observed that in symmetrical case, i.e. when all of the cavity regions are filled with biomolecule then interchanging the drain and source contact seems to have no effect on sensitivity. However, a significant change in sensitivity can be found as we modify the position and percentage of cavity region filled by biomolecules. For example, when only Region I and Region IV contain a biomolecule, then sensitivity is markedly higher for the first configuration (where Region IV is connected to the drain) than the second case (where Region I is connected to the drain). Similarly, the sensitivity is significantly higher for the first configuration (Region IV connected to drain) when the only cavity in Region I contains biomolecule. However, an opposite trend is observed for the cases where either one or both of Region III and IV are filled with biomolecule while Region I does not capture biomolecule. In these two cases actually, the second configuration (Region I connected to drain) exhibits better sensitivity compared to the first one. In summary, it can be concluded from the above findings that for identical fill in factor of biomolecules in the cavity region.

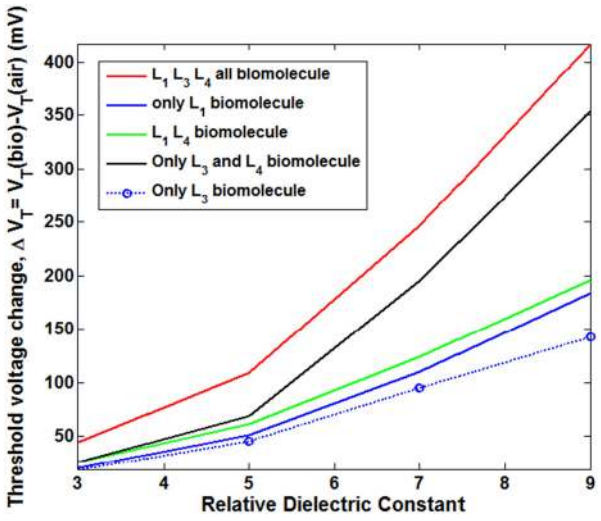

Fig. 7. Variation of sensitivity factor *ΔVth* for n-type DM-DG-MOSFETs for different position of biomolecule in the cavity region when Region I is connected to drain.

- The greater the distance of the center of a biomolecule from the drain end, higher the sensitivity of the device.

From the above study, we can get various sensitivities for two different configurations for same fill-in factor as shown in Fig. 8. Positioning of biomolecule closest to the middle of the channel and farthest away from the drain result in the highest sensitivity for a particular fill-in factor and vice versa. This study justifies the need to research further on these critical factors.

6. Conclusion

In this work, n-type Si JL-DM-DG-MOSFET has been investigated for the biosensing application in a dry environment. An analytical drain current model has been used and surface potential has been verified with 'SILVACO ATLAS' device simulation tool. N-type JL-DM-DG-MOSFET shows good change in threshold voltage with the modification of biomolecules' dielectric constant. The position of biomolecules and fill in factor of nanogap cavity have been varied to find out their effects on sensitivity. It has been found that maximum sensitivity could be obtained when all of the cavity regions are filled with a biomolecule. Moreover, for cavity areas with a partially filled biomolecule, the sensitivity

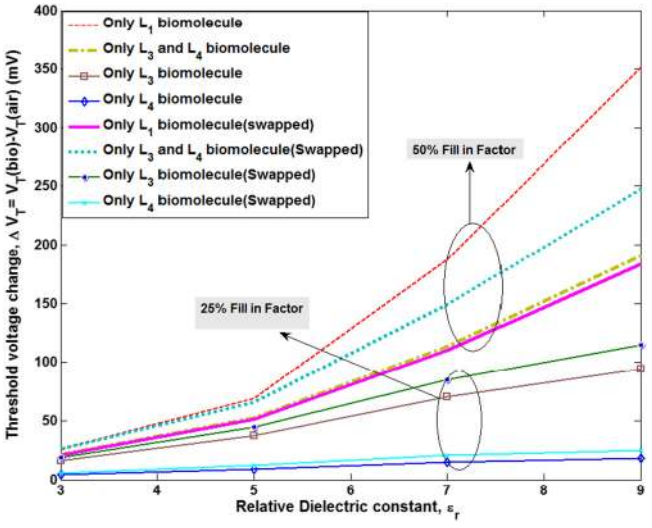

Fig. 8. Four different sensitivity profiles for same fill-in factor with interchange of drain and source contact.

can be enhanced by moving the biomolecules more towards the center of the channel and farther from the drain side.

References

[1] M. Waleed Shinwari, M. Jamal Deen, D. Landheer, Study of the electrolyte-insulator-semiconductor field-effect transistor (EISFET) with applications in biosensor design, Microelectron. Reliab. 47 (12) (2007) 2025–2057.

[2] M.C. Pirrung, How to make a DNA chip, Angew. Chemie - Int. Ed. 41 (8) (2002) 1276–1289.

[3] P. Ir, P.B. Em, F. Ee, ISFET, Theory and Practiceno. October 2003 1–26.

[4] J. Go, P.R. Nair, B. Reddy, B. Dorvel, R. Bashir, M.A. Alam, Beating the Nernst limit of 59 mV/pH with double-gated nano-scale field-effect transistors and its applications to ultra-sensitive DNA biosensors, Tech. Dig. - Int. Electron Devices Meet. IEDM 2 (2010) 202–205.

[5] M.J. Spijkman, J.J. Brondijk, T.C.T. Geuns, E.C.P. Smits, T. Cramer, F. Zerbetto, P. Stoliar, F. Biscarini, P.W.M. Blom, D.M. De Leeuw, Dual-gate organic field-effect transistors as potentiometrie sensors in aqueous solution, Adv. Funct. Mater. 20 (6) (2010) 898–905.

[6] Abir Shadman, Ehsanur Rahman, Quazi D.M. Khosru, Monolayer MoS_2 and WSe_2 double gate field effect transistor as super Nernst pH sensor and Nanobiosensor, Sens. Bio-Sens. Res. 11 (1) (2016) 45–51.

[7] Kanak Datta, Abir Shadman, Ehsanur Rahman, Quazi D.M. Khosru, Trilayer TMDC Heterostructures for MOSFETs and Nanobiosensors, J. Electron. Mater. 46 (2) (2017) 1248–1260.

[8] M.W.S.R.S. Cobbold, Basic properties of the electrolyte-SiO_2–Si system, IEEE Trans. Electron Devices (1) (1979) 1805–1815.

[9] E. Stern, R. Wagner, F.J. Sigworth, R. Breaker, T.M. Fahmy, M.A. Reed, Importance of the debye screening length on nanowire field effect transistor sensors, Nano Lett. 7 (11) (2007) 3405–3409.

[10] F. Puppo, M.-A. Doucey, T.S.Y. Moh, G. Pandraud, P.M. Sarro, G. De Micheli, S. Carrara, Femto-molar Sensitive Field Effect Transistor Biosensors Based on Silicon Nanowires and Antibodies, 2013 1–4.

[11] R. Narang Ajay, M. Gupta, M. Saxena, Investigation of dielectric-modulated double-gate junctionless MOSFET for detection of biomolecules, 2013 Annu. IEEE India Conf. INDICON, Vol. 2, 2013, pp. 1–6.

[12] C.W. Lee, A. Afzalian, N.D. Akhavan, R. Yan, I. Ferain, J.P. Colinge, Junctionless multigate field-effect transistor, Appl. Phys. Lett. 94 (5) (2009) 13–15.

[13] J.-P. Colinge, C.-W. Lee, A. Afzalian, N.D. Akhavan, R. Yan, I. Ferain, P. Razavi, B. O'Neill, A. Blake, M. White, A.-M. Kelleher, B. McCarthy, R. Murphy, Nanowire transistors without junctions, Nat. Nanotechnol. 5 (3) (2010) 225–229.

[14] C.W. Lee, A. Borne, I. Ferain, A. Afzalian, R. Yan, N. Dehdashti Akhavan, P. Razavi, J.P. Colinge, High-temperature performance of silicon junctionless MOSFETs, IEEE Trans. Electron Devices 57 (3) (2010) 620–625.

[15] F. Jazaeri, L. Barbut, A. Koukab, J.M. Sallese, Analytical model for ultra-thin body junctionless symmetric double gate MOSFETs in subthreshold regime, Solid. State. Electron. 82 (2013) 103–110.

[16] S. Kim, J.H. Ahn, T.J. Park, S.Y. Lee, Y.K. Choi, A biomolecular detection method based on charge pumping in a nanogap embedded field-effect-transistor biosensor, Appl. Phys. Lett. 94 (24) (2009) 1–4.

[17] K.-W. Lee, S.-J. Choi, J.-H. Ahn, D.-I. Moon, T.J. Park, S.Y. Lee, Y.-K. Choi, An underlap field-effect transistor for electrical detection of influenza, Appl. Phys. Lett. 96 (3) (2010) 33703.

[18] H. Im, X.-J. Huang, B. Gu, Y.-K. Choi, A dielectric-modulated field-effect transistor for biosensing, Nat. Nanotechnol. 2 (7) (2007) 430–434.

[19] R. Narang, M. Saxena, M. Gupta, Comparative analysis of dielectric-modulated FET and TFET-based biosensor, IEEE Trans. Nanotechnol. 14 (3) (2015) 427–435.

[20] R. Narang Ajay, M. Saxena, M. Gupta, Analysis of gate underlap channel double gate MOS transistor for electrical detection of bio-molecules, Superlattice. Microst. 88 (2015) 225–243.

[21] R. Ajay, M. Saxena Narang, M. Gupta, Drain current model of a four-gate dielectric modulated MOSFET for application as a biosensor, IEEE Trans. Electron Devices 62 (8) (2015) 2636–2644.

[22] R. Narang Ajay, M. Saxena, M. Gupta, Investigation of dielectric modulated (DM) double gate (DG) junctionless MOSFETs for application as a biosensors, Superlattice. Microst. 85 (2015) 557–572.

[23] R. Narang, S.S. Member, M. Saxena, S.S. Member, Dielectric modulated tunnel field-effect transistor — a biomolecule sensor. IEEE Electron Device Lett. 33 (2) (2012) 266–268.

[24] C. Kim, J. Ahn, K. Lee, C. Jung, H.G. Park, Y. Choi, A new sensing metric to reduce data fluctuations in a nanogap-embedded field-effect transistor biosensor. IEEE Trans. Electron Devices, 59 (10) (2012) 2825–2831.

[25] K.-W. Lee, S.-J. Choi, J.-H. Ahn, D.-I. Moon, T.J. Park, S.Y. Lee, Y.-K. Choi, An underlap field-effect transistor for electrical detection of influenza, Appl. Phys. Lett. 96 (3) (2010) 33703.

[26] http://www.silvaco.com/products/tcad/device_simulation/atlas/atlas.html.

[27] S. Busse, V. Scheumann, B. Menges, S. Mittler, Sensitivity studies for specific binding reactions using the biotin/streptavidin system by evanescent optical methods, Biosens. Bioelectron. 17 (8) (2002) 704–710.

[28] D.-X. Xu, A. Densmore, S. Janz, P. Waldron, T. Mischki, G. Lopinski, A. Delâge, P. Cheben, J. Lapointe, B. Lamontagne, J.H. Schmid, Spiral-path high-sensitivity silicon photonic wire molecular sensor with temperature-independent response, Opt. Lett. 33 (6) (2008) 596–598.

[29] E. Makarona, E. Kapetanakis, D.M. Velessiotis, A. Douvas, P. Argitis, P. Normand, T. Gotszalk, M. Woszczyna, N. Glezos, Vertical devices of self-assembled hybrid organic/inorganic monolayers based on tungsten polyoxometalates, Microelectron. Eng. 85 (5–6) (2008) 1399–1402.

[30] S. Kim, D. Baek, J.Y. Kim, S.J. Choi, M.L. Seol, Y.K. Choi, A transistor-based biosensor for the extraction of physical properties from biomolecules, Appl. Phys. Lett. 101 (7) (2012).